Biophysical Chemistry 136 (2008) 38–43

Contents lists available at ScienceDirect

Biophysical Chemistry

journal homepage: http://www.elsevier.com/locate/biophyschem

Photostability of green and yellow fluorescent proteins with fluorinated chromophores, investigated by fluorescence correlation spectroscopy

S. Veettil [a], N. Budisa [b], G. Jung [a,*]

[a] Biophysical Chemistry, Saarland University, Building B2.2, D-66123, Saarbruecken, Germany
[b] Max-Planck-Institute for Biochemistry, Am Klopferspitz 18a, D-82152 Martinsried, Germany

ARTICLE INFO

Article history:
Received 19 March 2008
Received in revised form 10 April 2008
Accepted 10 April 2008
Available online 23 April 2008

Keywords:
Autofluorescent protein
Fluorinated tyrosine
Photostability
Fluorescence correlation spectroscopy
Electron transfer reactions
Photobleaching

ABSTRACT

The photostability of the widely used autofluorescent proteins EGFP and EYFP and their fluorinated counterparts were compared by means of fluorescence correlation spectroscopy. We analyzed the reduction of the apparent diffusional time in analogy to fluorescence quenching in which the 'photon concentration' is treated as the quencher concentration.
The quantum yields of photobleaching Φ_{bl} of EYFP (6.1×10^{-5}) and EGFP (8.2×10^{-5}) are in agreement with the previously published values. Among the investigated mutants, EYFP has the highest photostability and there is an enhanced photobleaching in (2-F) Tyr-EYFP. It turns out that the chromophore fluorination has no significant influence on the photostability.

1. Introduction

In the past dozen years, Autofluorescent Proteins (AFPs) became indispensable tools in life sciences [1]. The importance emerged from their fluorescence which forms spontaneously from the amino acid chain without the need of cofactors or modifying enzymes [2]. The discovery of coral chromoproteins with unique photophysical properties led to a tremendous increase in their use in all areas of fluorescence based technology [3]. In microscopy, their usage ranges from multicolour labelling of cell compartments via quantifying physiological parameters by FRET-approaches to tracing and counting of tagged proteins by single-molecule detection schemes [4]. However, especially those applications which require high excitation intensities suffer from the limited fluorescence survival time of these proteins. Photodestruction of the chromophore is assumed to be the main reason for fluorescence interruption, although it was shown that fluorescence was recovered by the decay of exceptionally long-living dark states [5]. Photobleaching therefore subsumes these processes, and the molecular quality "photostability" characterizes the different AFPs to withstand them. Deciphering the molecular basis for the underlying chemical transformations might assist to overcome those limitations. Comparative investigations of different AFPs, which were successfully applied to unravel pathways of internal conversion and excited-state proton transfer, ought to support the finding of molecular mechanisms of photobleaching [6,7]. The strategy here relies on the modification of the chromophore by fluorination thereby circumventing the limited variety of natural chromophore structures with similar electronic transition energies. In the present study, global replacement of tyrosine by 2-fluorotyrosine, i.e. (2-F)-Tyr and 3-fluorotyrosine, i.e. (3-F)-Tyr in EGFP and EYFP mutants, were produced in Tyr-auxotrophic *E. coli* strains [8,9]. Due to the different electronic properties of C–F bond compared to the C–H bond, the replacement of hydrogen with fluorine in AFP chromophores is expected to be accompanied by differences in their optical properties [10].

Measuring the photostability of fluorophores which are principally appropriate for single-molecule research imposes practical problems. Imaging techniques are based on the analysis of detected fluorescence photons but require good statistics to average out orientational heterogeneities [11]. Furthermore, if immobilized molecules are analyzed, the influence of the support has to be considered. Experiments in the fluid phase, notably Fluorescence Correlation Spectroscopy (FCS), were used to determine the photostability of fluorescent dyes [12–14]. In FCS, photodestruction appears as a reduction of the residence time in the detection volume. Despite the easy performance of FCS, the analysis of photostability is hampered by the excitation profile of a strongly focused laser beam, which is spatially inhomogeneous: it has a Gaussian intensity profile perpendicular to the beam direction and has a Lorentzian intensity profile along the propagation direction. With no photobleaching occurring, an intensity dependent increase of the diffusional time can be

* Corresponding author. Tel.: +49 68130264848; fax: +49 68130264846.
E-mail address: g.jung@mx.uni-saarland.de (G. Jung).

0301-4622/$ – see front matter © 2008 Elsevier B.V. All rights reserved.
doi:10.1016/j.bpc.2008.04.006

discerned under these excitation conditions [15]. This experimental observation is ascribed to fluorescence saturation in the central part of the detection focus and a concomitantly stronger contribution of out-of-focus parts to the correlation curve. Furthermore, a practical, analytical solution for the combination of diffusion and photobleaching is not available yet.

In the present work, the mentioned shortcomings of FCS are circumvented by a careful experimental design, consideration of saturation effects and a comparative analysis of the photostability. After the section 'Materials and methods' we sketch our analysis of the photostability based on FCS measurements. These data which were obtained for GFP and YFP with differently fluorinated chromophores, are presented and discussed.

2. Materials and methods

2.1. Samples

EGFP was obtained from Clontech. The fluorinated proteins were produced as described previously and were concentrated to a final concentration of ~1 mg/ml [8]. Small quantities were serially diluted in a buffer at pH 10 (HPCE-grade, Fluka) to micromolarity for fluorescence spectra and to the nanomolar range for the FCS experiments. A drop of such a solution was put on top of a silanized cover slide with specified thickness of 0.17 mm. The high pH was chosen to avoid complications due to external protonation as described before [16].

2.2. Fluorescence excitation and emission spectra

Fluorescence excitation emission spectra were taken with a commercial fluorescence spectrometer (Jobin Yvon-SPEX Instrument S.A, Inc.) at pH 10. The optical resolution of the spectra was 1 nm. Excitation spectra were corrected by use of a highly concentrated rhodamine B solution as reference quantum counter [17].

2.3. Microscopic setup

Experiments were performed with a home-built confocal setup based on an inverted microscope (Axiovert 200, Zeiss). At the beginning, an Ar-ion laser, operating at λ_{exc}=488 nm (Innova I-304 C, Coherent), was coupled into an optical fibre and outcoupled by a 40x objective lens resulting in a parallel laser beam with a diameter of 0.8 mm. In the course of the described experiments, the above mentioned laser was replaced by a frequency-doubled diode laser (Picarro, Soliton), also operating at λ_{exc}=488 nm with a diameter of 0.7 mm. The laser beams were directed to the microscope body without the use of further lenses, and there deflected by a dichroic mirror (495 DRLP, Omega). The laser was focussed to a spot of focal width ω_0~440 nm by a water immersion objective lens (63x NA 1.2 WI, Zeiss). Fluorescence was collected by the same objective and was focussed by the tube lens to a pinhole with a diameter of 50 µm. After additional filtering with a bandpass filter (HQ 525/50, AHF Analysentechnik, for GFPs and HQ 583/120, AHF Analysentechnik, for YFPs), fluorescence was split by semitransparent mirror and detected by two avalanche photodiode modules (SPCM-14-AQR, PerkinElmer Optoelectronics). TTL-signals, each corresponding to a detected photon, were cross-correlated by a hardware correlator (FLEX 02 D, www.correlator.com) finally yielding the autocorrelation function with nanosecond time resolution. Correlation curves were recorded depending on the applied excitation intensity in the range between 12 and 259 kW cm^{-2}.

2.4. Analysis of FCS data

Intensity dependent FCS data were analyzed according to Eq. (1) by means of commercial software (Origin Pro 7.5, Origin Lab, MA, USA). All depicted autocorrelation curves were normalized with respect to the number of molecules in the detection volume N (Fig. 1).

$$g^2(\tau) = 1 + \frac{1}{N}\left(\frac{1}{1+\left(\frac{\tau}{\tau_d}\right)}\right)[1 + C\cdot\exp(-k\tau)] \quad (1)$$

In this so-called two-dimensional model, which is valid for the pinhole diameter used here [18], only the diffusion perpendicular to the propagating laser is made responsible for fluorescence fluctuations and photobleaching appears as a reduction of the apparent diffusional time τ_d. The contrast C in Eq. (1) is the amplitude for the fast decaying part of the autocorrelation curves with k as the rate constant for the fluorescence fluctuations. Its decay constant reflects the time scale upon which typical on–off transitions take place. C is of importance in discussing photostability as it can be related to the fraction of molecules in a dark state, [D], according to Eq. (2) [19].

$$\frac{[D]}{1-[D]} = C \rightarrow [D] = \frac{C}{1+C} \quad (2)$$

The larger [D], the less the time the molecules can spend in a chromophore state where they can be excited and possibly undergo photodestruction. The bright fraction [B] is related to [D], [B]=1−[D].

3. Analysis of the photostability

A reduction of τ_d is a hallmark of ongoing photobleaching while molecules diffuse through the detection volume (Fig. 3 a). Several attempts were made to allow for this experimental observation [12–14,20]; formal splitting of the entity of fluorescent molecules into two fractions, one part corresponding to surviving molecules and the other part to bleached molecules, became most widespread, although recent results indicate some arbitrariness in this model [21]. The model which we apply here is based on the idea that interruption of a molecule's fluorescence emission can be due to photobleaching or leaving the detection volume. Both processes are treated as competing pathways following ordinary chemical kinetics with k_{bl}^{eff} as the effective (intensity dependent) rate constant for photobleaching and

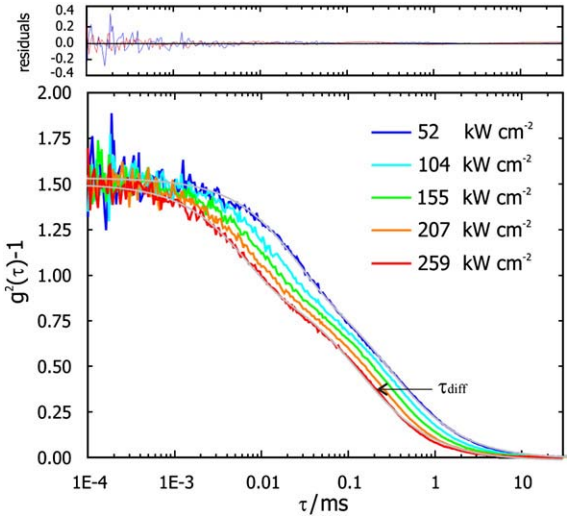

Fig. 1. Intensity dependent fluorescence correlation curves for EYFP at pH 10 (λ_{exc}=488 nm). Different excitation intensities are shown in the graph with corresponding colours. A strong reduction in apparent diffusion time upon increasing excitation intensity is observed. For better comparability, all FCS data are normalised. Residual plot for the fit (52 kW cm^{-2}-blue line, 259 kW cm^{-2}-red line) is also shown in the figure. (For interpretation of the references to colour in this figure legend, the reader is referred to the web version of this article.)

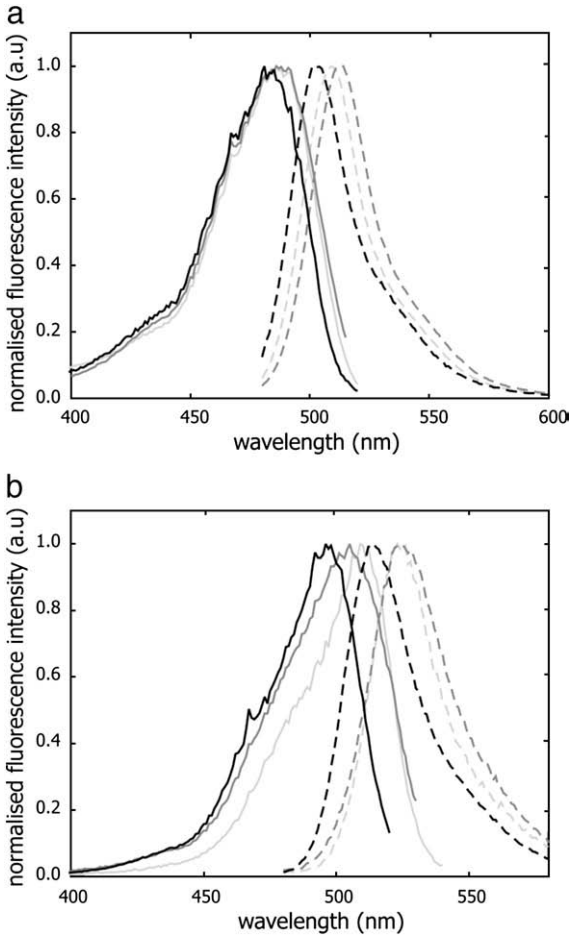

Fig. 2. a) Normalised fluorescence excitation (full line) and emission (broken line) spectra of GFP variants at pH 10. EGFP is printed in light grey and (3-F)-Tyr-EGFP and (2-F)-Tyr-EGFP are printed in grey and black respectively. b) Normalised fluorescence excitation (full line) and emission (broken line) spectra of YFP variants at pH 10. EYFP is printed in light grey and (3-F)-Tyr-EYFP and (2-F)-Tyr-EYFP are printed in grey and black respectively.

$1/\tau_0$ as "intrinsic rate constant" for diffusion. The measured intensity dependent τ_d is therefore composed of both contributions in Eq. (3).

$$\frac{1}{\tau_d} = \frac{1}{\tau_0} + k_{bl}^{eff} \tag{3}$$

In the simplest approach, k_{bl}^{eff} is proportional to the number of excitation cycles, k_{12} (Eq. (4)).

$$k_{bl}^{eff} = \phi_{bl} \cdot k_{12} = \phi_{bl} \cdot \sigma \cdot \left(\frac{I}{h\nu}\right) = \sigma_{bl} \cdot \left(\frac{I}{h\nu}\right) \tag{4}$$

The proportionality constant is the quantum yield of photobleaching Φ_{bl}. k_{12} is composed of the excitation intensity I, the photon energy $h\nu$ and the absorption cross section σ. The bleaching cross section σ_{bl} is the product of Φ_{bl} and σ.

The situation is comparable to fluorescence quenching, where the nonradiative decay of an excited state is promoted by collisions with the quencher. Experimentally, this can be detected by a reduction of the fluorescence lifetime. It is therefore straightforward to analyze the (fluorescence) survival time in a similar manner in which the "photon concentration", $c_{photons}$ is treated as the quencher concentration in fluorescence quenching. The unusual expression "photon concentration" is the number of photons per area and time. It is equal to the intensity I divided by the photon energy $h\nu$ and is therefore related to

Table 1
Spectral data for EGFP, EYFP and their variants

Protein	Tsien, 1998 [31]	Pal et al., 2005 (pH 7) [8]			This work (pH 10)	
	ε_M (λ_{max})	ε_M (λ_{max})	λ_{exc}	λ_{em}	λ_{exc}	λ_{em}
EGFP	55,000–57,000	34,340	488	510	486	509
(2-F) Tyr-EGFP		22,190	482	504	481	501
(3-F) Tyr-EGFP		30,200	485	514	486	512
EYFP	83,400	48,770	514	527	509	523
(2-F) Tyr-EYFP		55,460	504	520	496	514
(3-F) Tyr-EYFP		48,790	518	533	505	524

Molar extinction coefficient (ε_M) is expressed in M^{-1} cm^{-1}. Fluorescence excitation (λ_{exc}) and emission (λ_{em}) values are in nanometers.

k_{12}. The analysis is performed in a Stern–Volmer-like plot (Eq. (5), Fig. 3 b).

$$\frac{\tau_0}{\tau_d(I)} = 1 + \frac{\sigma_{bl} \cdot \tau_0}{h\nu} \cdot I = 1 + \sigma_{bl} \cdot \tau_0 \cdot c_{photons} \tag{5}$$

The intrinsic diffusional time τ_0 can be computed phenomenologically by extracting the amplitude of the decaying exponential function of $\tau_d(I)$ (Fig. 3 a). From the slope of $\tau_0/\tau_d(I)$ versus the intensity I (Fig. 3 b), the bleaching cross section σ_{bl} divided by the photon energy $h\nu$, is obtained by the subsequent division with τ_0 (Fig. 4 a). τ_0 is used here for

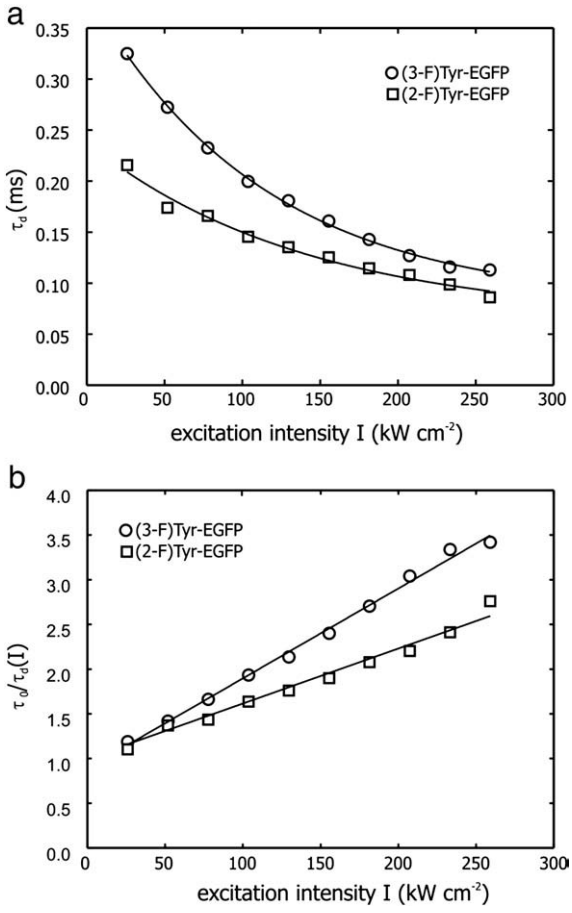

Fig. 3. a) Intensity dependent τ_d of (3-F) Tyr-EGFP (○) and (2-F) Tyr-EGFP (□), (λ_{exc}=488 nm) with phenomenological fitting for the determination of $\tau_{d,0}$. A strong decay of τ_d with increasing excitation intensity indicates photobleaching, but seems to level off at high intensities. b) Linear plot of τ_0/τ_d (I) versus Intensity I of (3-F)-Tyr-EGFP (○) and (2-F)-Tyr-EGFP (□). Photobleaching kinetics can be analyzed in a 'Stern–Volmer' like plot. The slope of the fitting line is proportional to the rate constant of photobleaching.

the sake of clearness and to stress the similarity of the analytical approach to fluorescence quenching.

4. Results and discussion

4.1. Spectral characteristics

Spectra were recorded at pH 10, where the FCS experiments were performed. Excitation and emission maxima of (2-F)-Tyr proteins were blue shifted compared to both the parent proteins and the (3-F)-Tyr-EYFP (Fig. 2). Agreement between our data and previously published values were found for all EGFPs (Table 1). Differences in the fluorescence emission maxima and excitation maxima were noticed for the red-shifted EYFPs. These differences might results from a partial deprotonation of Tyr203, (2-F)-Tyr203 and (3-F)-Tyr203 at the pH-value of our study, which is above the pK_a of these amino acids [22]. Such altered π–π interactions might result in a weakened red-shift of the spectra at pH 10 compared to the values at pH 7. Changes might also be due to the presence of multiple protonation sites which is recently described [23]. Relevant for our work, however, is that the relative excitation cross section σ_{exc}^{rel} at λ=488 nm, related to the excitation maximum, is nearly constant for all GFPs. σ_{exc}^{rel} are lower for the YFPs due to their red-shifted excitation maxima. The reason why we use the dimensionless σ_{exc}^{rel} instead of σ (in units of $Å^2 = 10^{-16}$ cm^2) is that no reliable values for σ of single fluorescent proteins exist. All published extinction coefficients (see Table 1) suffer from the fact that incomplete chromophore formation results in spectroscopically silent absorbance in the visible range whereas the protein absorption at λ=280 nm, which is used as reference, is not affected. Despite this uncertainty, most published data match with excitation cross sections which are larger for YFP than for GFP by about 50% [24].

4.2. Photostability determination

Several photobleaching pathways of highly fluorescent molecules are discussed, among which one-electron photooxidation and photo-oxygenation are most prominent [25]. In the case of the autofluorescent proteins, the situation is more complex as the chromophore is shielded by the protein barrel. Recent results, however, indicate that oxygen can easily access the chromophore [26]. The existence of long-living dark states and an electron transfer reactions leading to photoconversion further complicate the photochemistry of this protein class [6,27]. Chemical modifications for studying these mechanisms became possible by implementing unnatural amino acids which resulted in chromophore fluorination [8,9]. Previously, fluorotyrosines were used to unravel reactions which involve radicals [28]. The kinetics of electron transfer processes were altered due to the change of the redox potentials upon fluorination with respect to the natural counterpart. (3-F)-Tyr, which also finds application here, roughly reduced the kinetics of the investigated electron transfer reaction by a factor of 3. Although experimental data on the redox potentials of the chromophore and its fluorinated derivatives are not available to our knowledge, at least a qualitative change of the photostability is expected upon chromophore fluorination when electron transfer reactions substantially contribute to the photobleaching of AFP.

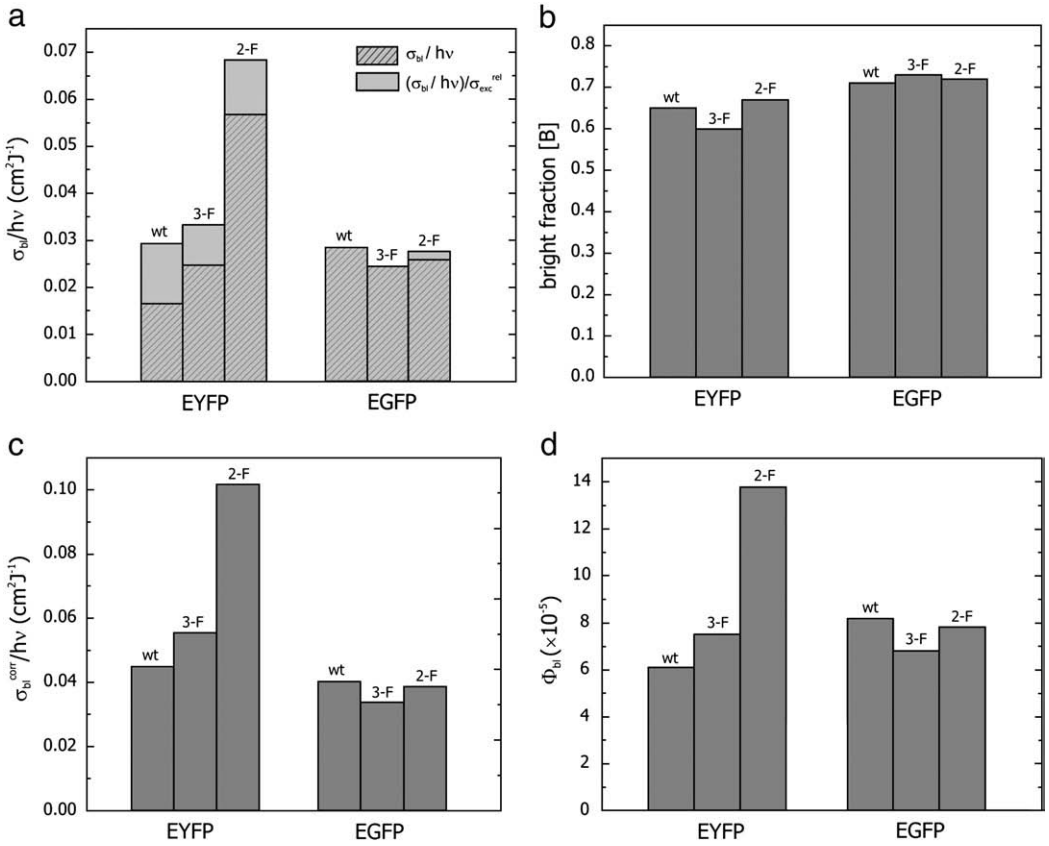

Fig. 4. a) Photostability profile of investigated GFP and YFP variants. The bleaching cross section σ_{bl} (divided by the photon energy $h\nu$) is obtained from the linear fitting of Fig. 3 b and division with $\tau_{d,0}$. $\sigma_{bl}/h\nu$ after correction with the relative excitation cross section σ_{exc}^{rel} is also shown in the graph. b) The bright fraction [B] of all the investigated mutants. It is calculated from the dark fraction [D]. The contrast C is a measure of the dark state population [D] under photostationary conditions. c) Comparison of the different $\sigma_{bl}^{corr}/h\nu$ of EGFPs and EYFPs. $\sigma_{bl}^{corr}/h\nu$ is obtained by dividing $\sigma_{bl}/h\nu$ with relative excitation cross section σ_{exc}^{rel} and bright fraction [B]. d) Quantum yield of photobleaching Φ_{bl} of all the analyzed mutants. Φ_{bl} is obtained by dividing σ_{bl}^{corr} by σ (2 Å^2 for EGFPs and 3 Å^2 for EYFPs are taken), see Eq. (4). Φ_{bl} of EGFP (8.2×10^{-5}) and EYFP (6.1×10^{-5}) are in agreement with the previously published results.

In the investigated intensity range, all FCS curves could be fitted by Eq. (1). Even at moderate intensities, the contrast C is constant and independent of further intensity increase. Such behaviour indicates light-driven *cis–trans* isomerization [29,30]. This is also true for the fluorinated proteins in this study; however, the absolute values of C and accordingly $[B]$ differ (Eq. (2)). The photostability of the different fluorescent proteins to our disposal were determined as described in Section 3. All curves, as depicted in Fig. 3 b, exhibited a linear dependence on the applied intensity. This finding suggests that photobleaching manifests as a one-photon process. The bleaching cross section σ_{bl} is determined according to Eq. (5) by dividing the slope in Fig. 3 b by τ_0 and multiplying the photon energy, $h\nu$.

Unexpectedly, the experimentally accessible bleaching cross section σ_{bl} of 5 out of 6 investigated fluorescent proteins lie in the same range (Fig. 4 a). Only (2-F)Tyr-EYFP exhibits a faster bleaching. However, corrections have to be performed before conclusions about the relative photostability can be drawn. The bleaching cross section σ_{bl} depends on the relative absorption cross section σ_{rel} as it matters whether fluorophores are excited close to their maximum like the GFPs or in the blue wing of the absorption band like in the YFPs. The grey area in Fig. 4 a, shifted to higher values, accommodate for this. Not all proteins of one mutant are in a bright state but undergo isomerization into dark states. As in a previous study, we refer σ_{bl} to the bright fraction B which can be calculated by the contrast C [19] (Fig. 4 b).The more often the molecules resides in a dark state, the less likely it undergoes photodestruction. To account for this we divide $\sigma_{bl}/(h\nu\cdot\sigma_{exc}^{rel})$ by the bright fraction B (Fig. 4 c).

After these corrections, the situation is only slightly changed: all EGFPs have similar σ_{bl}^{corr} (within an estimated relative error of <20% from repeated experiments on some mutants), but still lower σ_{bl}^{corr} than the YFP counterparts. However, in EGFPs the fluorination enhances photobleaching especially in (2-F) Tyr-EYFP. Interestingly, the pH-dependence of its absorbance spectra deviated from the other fluorinated proteins resulting in a pK_a close to the parent protein [8]. This is noteworthy as the acidity of tyrosine is increased upon fluorination [22]. Facilitated access of protons to the chromophore might be the result of structural rearrangements which can also lead to a reduced shielding from molecular oxygen. The same might be true, however, to a lesser extent for (3-F) Tyr-EYFP. Our observations substantiate that some disturbances occur in the chromophore upon fluorination, the rate limiting step is probably not the putative electron transfer to molecular oxygen [26].

4.3. Comparison to previously determined values

So far, the relative photostability among the different proteins was discussed and revealed that the bleaching cross section of the investigated EGFP variants is smaller in comparison with the EYFP variants. Assigning the commonly accepted values of σ(~2 Å^2 for EGFP and ~3 Å^2 for EYFP) yields $\Phi_{bl}\sim 6.1\times10^{-5}-8.2\times10^{-5}$ according to Eq. (4) for all proteins [31] except (2-F) Tyr-EYFP (see Fig. 4 d). These values are only slightly higher than the reported values for EGFP and EYFP, measured by single-molecule fluorescence microscopy [11]. Note that the fluorescence quantum yield for EYFP is higher than for EGFP making EYFP even more favourable for fluorescence applications [19]. In addition, the photon detection probability is not uniform across the (inhomogeneous) excitation profile. It is, however, noteworthy that the saturation effects due to triplet population described in Ref. [15] are likely not having impact on the photostability measurements of autofluorescent proteins since here both forward and backward transitions to dark states are light-driven.

5. Conclusion

Reduced Φ_{bl} strongly suggests that EYFP has the highest photostability among the investigated mutants. In contrast to the stabilization effect of fluorination of fluorescent dyes [32], chromophore fluorination did not enhance the photostability advantageously. We assume that fluorination dislocates the protein folding or the molecular structure resulting in a reduced shielding and the formation of reactive oxygen species [26]. This might be tested by quantifying the singlet oxygen production. The absolute quantum yields for photostability, although similar to previously published values, should be interpreted with care as new analytical ways are yet to be developed for taking the detection nonlinearities in FCS into account.

Acknowledgement

This work was supported by the German Science Foundation (DFG, project JU-650/1-1) and BioFuture Program of the Federal Ministry of Education and Research of Germany. We also indebted to Babette Hinkeldey for critical reading of the manuscript.

References

[1] K.F. Sullivan, S.A. Kay, (eds.) Green fluorescent proteins, Methods Cell Biol. 58 (1999) 1–369.
[2] M. Chalfie, Y. Tu, G. Euskirchen, W.W. Ward, D.C. Prasher, Green fluorescent protein as a marker for gene expression, Science 263 (1994) 802–805.
[3] V.V. Vladislav, K.A. Lukyanov, The molecular properties and applications of Anthozoa fluorescent proteins and chromoproteins, Nat. Biotechnol. 22 (2004) 289–296.
[4] X.S. Xie, J. Yu, W.Y. Yang, Living cells as test tubes, Science 312 (2006) 228–230.
[5] G. Jung, J. Wiehler, W. Göhde, J. Tittel, T. Basché, B. Steipe, C. Bräuchle, Confocal microscopy of single molecules of the green fluorescent protein, Bioimaging 6 (1998) 54–61.
[6] G. Jung, J. Wiehler, A. Zumbush, The photophysics of green fluorescent protein: influence of the key amino acids at position 65, 203, and 222, Biophys. J. 88 (2005) 1932–1947.
[7] A. Kummer, H. Wiehler, H. Rehaber, C. Kompa, B. Steipe, M.E. Michel-Beyerle, Effect of threonine 203 replacements on excited-state dynamics and fluorescence properties of green fluorescent protein (GFP), J. Phys. Chem. B. 104 (2000) 4791–4798.
[8] P.P. Pal, J.H. Bae, M. K Azim, P. Hess, R. Friedrich, R. Huber, L. Moroder, N. Budisa, Structural and spectral response of *Aequorea victoria* green fluorescent proteins to chromophore fluorination, Biochemistry 44 (2005) 3663–3672.
[9] J.H. Bae, P. P Pal, L. Moroder, R. Huber, N. Budisa, Crystallographic evidence for isomeric chromophores in 3-fluorotyrosyl-green fluorescent protein, ChemBioChem 5 (2004) 720–722.
[10] N. Budisa, P.P. Pal, S. Alefelder, P. Birle, T. Krywcun, M. Rubini, W. Wenger, J.H. Bae, T. Steiner, Probing the role of tryptophans in *Aequorea victoria* green fluorescent proteins with an expanded genetic code, Biol. Chem. 385 (2004) 191–202.
[11] G.S. Harms, L. Cogent, P.H.M. Lommerse, G.A. Blab, T. Schmidt, Autofluorescent proteins in single-molecule research: applications to live cell imaging microscopy, Biophys. J. 80 (2001) 2396–2408.
[12] C. Eggeling, A. Volkmer, C.A.M. Seidel, Molecular photobleaching kinetics of rhodamine 6G by one- and two-photon induced confocal fluorescence microscopy, ChemPhysChem 6 (2005) 791–804.
[13] J. Widengren, A. Chmyrov, C. Eggeling, P. A Löfdahl, C.A.M. Seidel, Strategies to improve photostabilities in ultrasensitive fluorescence spectroscopy, J. Phys. Chem. A. 111 (2007) 429–440.
[14] C. Eggeling, J. Widegren, R. Rigler, C.A.M. Seidel, Photobleaching of fluorescent dyes under conditions used for single-molecule detection: evidence of two-step photolysis, Anal. Chem. 70 (1998) 2651–2659.
[15] I. Gregor, D. Patra, J. Enderlein, Optical saturation in fluorescence correlation spectroscopy under continuous-wave and pulsed excitation, ChemPhysChem 6 (2005) 164–170.
[16] G. Jung, C. Bräuchle, A. Zumbusch, Two-color fluorescence correlation spectroscopy of one chromophore: application to the E222Q mutant of the green fluorescent protein, J. Chem. Phys. 114 (2001) 3149–3156.
[17] J. Yguerabide, Fast and accurate method for measuring photon flux in the range 2500–6000 Å, Rev. Sci. Instr. 39 (1968) 1048–1052.
[18] R. Rigler, Ü. Mets, J. Widengren, P. Kask, Fluorescence correlation spectroscopy with high count rate at low background: analysis of translational diffusion, Eur. Biophys J. 22 (1993) 169–175.
[19] G. Jung, A. Zumbusch, Improving autofluorescent proteins: comparative studies of the effective brightness of green fluorescent protein (GFP) mutants, Micros. Res. Techn. 69 (2006) 175–185.
[20] P. Dittrich, P. Schwille, Photobleaching and stabilization of fluorophores used for single-molecule analysis with one- and two-photon excitation, Appl. Phys. B. 73 (2001) 829–837.
[21] D. Satsoura, B. Leber, D. V Andrews, C. Fradin, Circumvention of fluorophore photobleaching in fluorescence fluctuation experiments: a beam scanning approach, ChemPhysChem 8 (2007) 834–848.
[22] B. Brooks, S.P. Robert, F.B. William, High-efficiency incorporation in vivo of tyrosine analogues with altered hydroxyl acidity in place of the catalytic tyrosine-

14 of Δ^5-3-ketosteroid isomerase of *Comamonas (Pseudomonas) testosteroni*: effects of the modifications on isomerase kinetics, Biochemistry 37 (1998) 9738–9742.
[23] R. Bizzarri, R. Nifosi, S. Abbruzzetti, W. Rocchia, S. Guidi, D. Arosio, G. Garau, B. Campanini, E. Grandi, F. Ricci, C. Viappiani, F. Beltram, Green fluorescent protein ground states: the influence of a second protonation site near the chromophore, Biochemistry 46 (2007) 5494–5504.
[24] G.A. Blab, P.H.M. Lommerse, L. Cognet, G.S. Harms, T. Schmidt, Two-photon excitation action cross-sections of the autofluorescent proteins, Chem. Phys. Lett. 350 (2001) 71–77.
[25] L. Song, E.J. Hennink, I.T. Young, H.J. Tannke, Photobleaching kinetics of fluorescein in quantitative fluorescence microscopy, Biophys. J. 68 (1995) 2588–2600.
[26] A. Jimenez-Banzo, S. Nonell, J. Hofkens, C. Flors, Singlet oxygen photosensitization by EGFP and its chromophore HBDI, Biophys. J. 94 (2008) 168–172.
[27] J.J. van Thor, T. Gensch, K.J. Hellingwerf, L.N. Johnson, Phototransformation of green fluorescent protein with UV and visible light leads to decarboxylation of glutamate 222, Nat. Struct. Biol. 9 (2002) 37–41.
[28] M.R. Seyedsayamdost, Y.R. Steven, G.N. Daniel, S. JoAnne, Mono-, Di-, and Tetra-substituted fluorotyrosines: New probes for enzymes that use tyrosyl radicals in catalysis, J. Am. Chem. Soc. 28 (2006) 1569–1579.
[29] P. Schwille, S. Kummer, A. A Heikal, W.E. Moerner, W.W. Webb, Fluorescence correlation spectroscopy reveals fast optical excitation-driven intramolecular dynamics of yellow fluorescent proteins, Proc. Natl. Acad. Sci. U S A. 97 (2000) 151–156.
[30] J. Widengren, P. Schwille, Characterisation of photo induced isomerisation and back isomerisation of the cyanine dye Cy5 by fluorescence correlation spectroscopy, J. Phys. Chem. A. 104 (2000) 6416–6428.
[31] R.Y. Tsien, The green fluorescent protein, Annu. Rev. Biochem. 67 (1998) 509–544.
[32] W.C. Sun, K.R. Gee, D.H. Klaubert, R.P. Haugland, Synthesis of fluorinated fluoresceins, J. Org. Chem. 62 (1997) 6469–6475.